Terrestrial Forcing of Marine Biodiversification

Ronald Martin (daddy@udel.edu)
University of Delaware
Andreas Cardenas
Universidad EAFIT https://orcid.org/0000-0003-3849-1514

Article

Keywords:

Posted Date: January 28th, 2022

DOI: https://doi.org/10.21203/rs.3.rs-1232652/v1

Abstract

Physical and biological factors have been proposed to account for the long-term development of marine biodiversity through the Phanerozoic Eon. Nutrient availability and primary productivity have, however, received less attention. We demonstrate that the diversification of the major marine faunas during the Phanerozoic was coupled to nutrient runoff from land and the diversification of phosphorus-rich plankton. Nutrient input to the oceans increased dramatically during the Meso-Cenozoic in response to widespread orogeny and peaked repeatedly following the eruption and weathering of phosphorus-rich continental Large Igneous Provinces. Widespread orogeny, forestation, and nutrient runoff during the Permo-Carboniferous was transitional to the Mesozoic and continued during the later Mesozoic and Cenozoic eras with the further tectonism and the spread of angiosperms, modern representatives of which tend to be more nutrient-rich. Early-to-middle Paleozoic diversity was, in contrast, limited by nutrient-poor plankton resulting from less frequent tectonism and poorly-developed terrestrial floras. Our results suggest that biodiversity on geologic time scales is unbounded, provided sufficient nutrients and nutrient-rich plankton are available on optimal timescales.

Introduction

Recent studies have produced relatively robust diversity patterns for the marine fossil record of the Phanerozoic Eon (last 542 million years) based largely on the Paleobiology Database (PBDB)[1-4]. This record confirms three main phases: the appearance and diversification of a relatively primitive Cambrian Fauna, the initial diversification of the Paleozoic Fauna and its subsequent plateauing (albeit with significant phases of diversification), and the nearly monotonic diversification of the Modern Fauna beginning in the Meso-Cenozoic era (Fig. 1). A broad range of physical and biological factors, likely acting and interacting on different scales of geologic time, have been hypothesized to explain the relative diversity of these three faunas, among them: sea level and habitat area associated with the tectonic forcing of sea level, changing climate regimes, latitudinal temperature gradients, biogeographic provinciality, oxygen levels, competition and predation, and biological disturbance[6-9].

Physical controls are also associated with orogeny and erosion, potentially implicating nutrient runoff, primary productivity, and related “trophic resources” (food, energy) in marine biotic turnover and diversification during the Earth’s history[10-14]. Such relationships between nutrient availability, primary productivity, and biodiversity are evident in the broad patterns of strontium isotopes and the fossil record of marine biodiversity during the Phanerozoic[11-14]. The steep rise of the Modern fauna coincides with a similar, more-or-less monotonic rise of strontium isotope ratios ($^{87}Sr/^{86}Sr$), reflecting the widespread orogeny of this interval (Fig. 1). Major increases in $^{87}Sr/^{86}Sr$ indicate continental collisions of the Himalayan type: orogeny delivers the heavier ^{87}Sr to the oceans in response to continental weathering, as opposed to ^{86}Sr associated with increased rates of seafloor spreading and hydrothermal weathering[15-16]. Strontium isotope ratios ($^{87}Sr/^{86}Sr$) have therefore been employed as a general proxy for both terrestrial runoff and associated nutrient input to the oceans[11-17]. This behavior is affirmed by the 9‰ rise of ^{87}Li in planktonic foraminifera from the Paleocene to present, consistent with uplift and more rapid continental denudation[18]. Trends for selenium, another indicator of oxidative weathering of continental rocks, tend to parallel strontium isotope trends curves, but correlate more strongly with trace elements, some of which are necessary for the photosynthetic machinery of phytoplankton, and also with phosphorus[19-20].

Volcanism, the associated injection of CO_2 and its acceleration of the hydrologic cycle via warming and weathering of volcanic rocks, as well as the input of volcanic ash have also been determined to be significant sources of nutrients on ecologic (natural and field experiments) and geologic scales of time[21-28]. The macronutrient phosphorus in particular is critical to the synthesis of cell membrane phospholipids, nucleic acids (DNA, RNA), and bone, and trophic groups belonging to higher levels of the pelagic food web are reported to grow increasingly nutrient and especially phosphorus-rich[29]. Phosphorus (as well as other nutrients such as silica) are initially largely derived from land by post-orogenic weathering by CO_2 of rocks of granitic composition and especially of mafic-to-intermediate volcanics and pyroclastics like those associated with Large Igneous Provinces (LIPs) and continental arcs[30-33]. Basaltic igneous rocks are reported to weather 5–10 times faster than granitic or gneissic material while mantle plume volcanism is estimated to contribute ~10% of the total outgassed CO_2 flux during LIP emplacement, continental

rifting from 20 to 70%, and volcanic arcs 10-30% to CO_2 [30-34]. However, phosphorus has an ecologically long residence time in the oceans (~50,000 yrs) and has no atmospheric source, so its total oceanic inventory is ultimately controlled by weathering, nutrient runoff, uptake into living and dead biomass, recycling, and authigenic precipitation during early diagenesis of organic matter in sediment pore water. Total phosphorus inventory is thus considered the ultimate limiting nutrient, setting the upper limit for marine primary productivity and the role of both in biodiversification on geologic time scales[35-37].

Significant correlations of the time series between biodiversification, LIP emplacement and the weathering of volcanic rocks, and geochemical indices should therefore occur, given that they likely interacted through biogeochemical cycles linking the major Earth systems of land, ocean, atmosphere, and biosphere.

Rationale And Results

We assessed the roles of phosphorus availability, primary productivity, and nutrient recycling on rates of nannofossil and marine genera origination rates (GOR) for the Meso-Cenozoic (Fig. 2)[38]. Besides strontium, detailed records of two other stable isotopes are also available for the Meso-Cenozoic: carbon ($\delta^{13}C$) and sulfur ($\delta^{34}S$). Both carbon and sulfur cycles control redox conditions at the Earth's surface. Carbon isotope ratios ($\delta^{13}C$) increase with increasing primary productivity but decrease with the decay of ^{12}C-rich dead organic matter, whereas sulfur isotope ratios ($\delta^{34}S$) reciprocate via the oxidation of dead organic matter by sulfate-reducing bacteria. Previously-published oceanic phosphorus accumulation rates (PAR) were used as a proxy for phosphorus availability[39].

Our analyses were conducted using uncorrected previously-published 11-myr binned data for stable isotopes and GOR and 5-myr bins at the approximate mid-points of 11-myr bins in an attempt to achieve finer temporal resolution within the temporal constraints of the raw data. Both 5- and 11-myr binned data for the Meso-Cenozoic yielded a significant Spearman's correlation ($p<0.05$) between $^{87}Sr/^{86}Sr$ and GOR, corroborating nutrient runoff in GOR, as previously reported for the entire Phanerozoic (Table 1)[12]. Strong significant correlations for both bin intervals were also found between biogenic PAR and GOR, directly implicating the bioavailability of phosphorus and its transfer along food chains in GOR. Five-myr binned data further yielded significant positive correlations which were found to be insignificant to marginally insignificant ($p<0.1$) to insignificant for 11-myr binned data: biogenic PAR with both total PAR and nannofossil diversification; total PAR with GOR; nannofossil diversification with GOR; and a significant negative correlation between $\delta^{13}C$ and $\delta^{34}S$. Both 5- and 11-myr binned data yielded marginally insignificant correlations between $\delta^{34}S$ and nannofossil diversification, while 5-myr binned data also detected weaker, marginally insignificant positive correlations between $\delta^{13}C$ and both nannofossil diversification ($p<0.085$) and GOR ($p<0.077$).

Table 1. Comparison of Correlations of Uncorrected Data*.

11-myr bin	CO_2	$^{87}Sr/^{86}Sr$	Biogenic PAR	Total PAR	Nanno Divers	$\delta^{13}C$	$\delta^{34}S$	GOR	Sea Level
CO_2		0.15795	0.6191	0.68079	**0.053748**	0.85201	0.2738	0.47378	0.18541
$^{87}Sr/^{86}Sr$	-0.39868		0.33313	0.34889	0.7346	0.54963	0.23592	**0.0062**	0.76328
Biogenic PAR	-0.2143	0.39522		**0.051711**	**0.089633**	0.35987	0.75203	**0.00724**	0.12364
Total PAR	0.12637	0.28295	**0.71429**		0.19441	0.66761	0.78895	**0.067292**	**0.011225**
Nanno Divers	**-0.52527**	0.099671	**0.64286**	0.38462		0.39192	**0.058637**	**0.0586**	0.493
$\delta^{13}C$	0.054945	0.17498	0.38095	0.13187	0.24835		0.74794	0.2207	**0.056154**
$\delta^{34}S$	0.31429	0.33888	-0.1429	-0.08242	**-0.51648**	-0.09451		0.9465	0.44563
GOR	-0.20879	**0.69105**	**0.88095**	**0.52198**	**0.51648**	0.34945	0.01978		0.20256
Sea Level	0.37582	0.088596	0.59524	**0.67582**	0.2	**0.52088**	0.22198	0.36264	

5-myr bin	CO_2	$^{87}Sr/^{86}Sr$	Biogenic PAR	Total PAR	Nanno Divers	$\delta^{13}C$	$\delta^{34}S$	GOR	Sea Level
CO_2		0.092295	0.46446	0.53194	**0.026636**	0.5898	0.35741	0.10304	**0.050857**
$^{87}Sr/^{86}Sr$	-0.31841		0.13407	0.46623	0.63687	0.6026	0.36151	**0.004704**	0.56479
Biogenic PAR	-0.19706	0.39118		**0.002854**	**0.023537**	0.3218	0.38036	**8.82E-07**	0.1919
Total PAR	-0.12576	0.14639	**0.69412**		**0.002661**	0.77617	0.63872	**0.000116**	**0.046842**
Nanno Divers	**-0.41133**	0.091503	**0.56176**	**0.55495**		**0.084763**	**0.054651**	**0.000106**	0.4535
$\delta^{13}C$	0.10443	0.10088	0.26471	0.057387	**0.32562**		**0.025269**	**0.076607**	**0.035143**
$\delta^{34}S$	0.17734	0.17585	-0.2353	0.094628	**-0.36059**	**-0.41478**		0.94742	0.6075
GOR	-0.30887	**0.51005**	**0.91176**	**0.67399**	**0.65764**	**0.33399**	-0.01281		0.53119
Sea Level	0.36601	-0.11148	0.34412	**0.38584**	0.14483	**0.39261**	-0.0995	0.12118	

***Data not corrected with Bonferroni correction (see below). Upper half: p (uncorrelated); lower half: ρ.**

Boldface blue: significant correlations (p<0.05); Boldface black: marginal correlations discussed in text.

Sea level exhibited no to possibly a marginal direct impact on GOR with either 11 or 5-myr binned data, similar to earlier findings for the 11-myr time scale (Table 1)[12]. Both binning methods, however, implicated sea level in total PAR and carbon burial ($\delta^{13}C$)

at significant to marginally-insignificant levels. Comparison of the sea level curve with those of other indices (Fig. 2) indicates that the flooding of shelves undoubtedly plays significant roles in biodiversification on akin to Sloss sequences (ca. tens-of-millions of years or more) and tectonic cycles by establishing the broad constraints of habitat availability on primary and secondary productivity ($\delta^{13}C$) and microbial sulfate reduction ($\delta^{34}S$) via substrate, sediment accumulation rates, oxygenation, depth and areal extent of the photic zone, and competition for light and nutrients[7,8,43-47].

Two sets of correlations were also conducted with the Bonferroni correction: one incorporating CO_2 and sea level and the other omitting them because of their lack of correlation with uncorrected data (Table 2)[38]. The Bonferroni correction has been widely recommended in some disciplines when conducting multiple comparisons. The correction has also been criticized; it is quite conservative and may erroneously reject null hypotheses or accept false ones and therefore is not used by some workers, who instead advocate using only uncorrected data[38]. Including all variables required a Bonferroni correction of p to ~0.0014, resulted in no significant correlations for 11-myr binned data and only a single correlation between biogenic PAR and GOR for 5-myr binned data ($\rho \approx 0.92$; p<3.2E-05); total PAR and nannofossil diversification also fell short of correlation with GOR with 5-myr binned data with the correction set to 0.0014 ($\rho \approx 0.67$, p<0.0042 and $\rho \approx 0.66$, p<0.0038, respectively; not shown). Excluding CO_2 and sea level yielded a somewhat higher p value of 0.0024 but this too yielded no significant correlations for 11-myr binned data; 5-myr corrected (0.0024) binned data that omitted CO_2 and sea level yielded significant correlations between $^{87}Sr/^{86}Sr$, biogenic and total PAR, and nannofossil diversification with GOR (Table 2). These correlations therefore appear robust, given the previous results for uncorrected data (p<0.05; cf. Tables 1, 2). They also suggest geologically rapid uptake of nutrients into living and dead biomass.

Cross-correlations of lagged indices against GOR weakened Spearman's correlations of both uncorrected and corrected data to insignificance, however, suggesting that the interactions of environmental forcings and the responses of biodiversification to them are occurring primarily on relatively geologically-short time scales ranging from 0-11 myr and even more strongly within the range of 0-5 myr.

Table 2. Comparison of correlations omitting CO_2 and sea level using Bonferroni correction*.

11-myr bin	$^{87}Sr/^{86}Sr$	Biogenic PAR	Total PAR	Nanno Divers	$\delta^{13}C$	$\delta^{34}S$	GOR
$^{87}Sr/^{86}Sr$		1	1	1	1	1	0.13025
Biogenic PAR	0.39522		1	1	1	1	0.15208
Total PAR	0.28295	0.71429		1	1	1	1
Nanno Divers	0.099671	0.64286	0.38462		1	1	1
$\delta^{13}C$	0.17498	0.38095	0.13187	0.24835		1	1
$\delta^{34}S$	0.33888	-0.1429	-0.0824	-0.5165	-0.0945		1
GOR	0.69105	0.88095	0.52198	0.51648	0.34945	0.01978	
5-myr bin	**$^{87}Sr/^{86}Sr$**	**Biogenic PAR**	**Total PAR**	**Nanno Divers**	**$\delta^{13}C$**	**$\delta^{34}S$**	**GOR**
$^{87}Sr/^{86}Sr$		1	1	1	1	1.00E+00	9.88E-02
Biogenic PAR	0.39118		0.059928	0.49428	1	1	1.85E-05
Total PAR	0.14639	0.69412		0.055883	1	1	0.002437
Nanno Divers	0.091503	0.56176	0.55495		1	1	0.002225
$\delta^{13}C$	0.10088	0.26471	0.057387	0.32562		0.53065	1
$\delta^{34}S$	0.17585	-0.2353	0.094628	-0.36059	-0.4148		1
GOR	0.51005	0.91176	0.67399	0.65764	0.33399	-0.01281	

*Bonferroni correction set to p<0.0024; upper half (above shaded boxes): p (uncorrelated);

lower half (below shaded boxes): ρ; dark blue: significant correlations (p<0.0024) [38].

Phytoplankton Stoichiometry Fueled Diversification of the Modern Fauna

Our results indicate that the initial diversification of the Modern Fauna is coupled to the appearance and diversification of new major planktonic taxa. The dominant eukaryotic plankton of the Meso-Cenozoic have been allied with so-called “red lineages” (coccolithophorids, dinoflagellates diatoms) characterized by the accessory pigment chlorophyll c and specific trace elements employed in their plastids and low carbon:phosphorus (C:P) ratios. Although their stoichiometry varies in response to natural conditions of temperature and nutrient availability, culture studies of modern representatives have been determined to be relatively phosphorus-rich and carbon-poor, and modeling of C:P occurring at the time of each major taxon’s appearance resembles that of their cultured modern representatives, suggesting that the nutrient preferences and stoichiometric compositions of modern representatives are evolutionarily conserved and reflect ancestral conditions rather modern ones[20,37]. Ecologic stoichiometric theory predicts that increasing the phosphorus content of phytoplankton decreases the amount of energy that consumers must expend to respire excess carbon to obtain inorganic macronutrients like phosphorus, potentially leaving excess resources like energy to be devoted to metabolic activity, reproduction, and changes in life cycles that could potentially impact diversification[29]. Calcareous plankton and the advent of deep-sea calcareous oozes linked tectonism to atmospheric carbon concentrations and weathering rates. A higher recycling efficiency between subducted carbon and CO_2 return flux to the atmosphere via volcanism, as occurred during the Meso-Cenozoic in the form of increasing deposition of

calcareous oozes would have provided positive feedback on volcanism and CO_2 flux to the atmosphere, enhancing weathering rates and nutrient input to the oceans, primary productivity, and calcareous plankton[34,48,49]. The apparent steep expansion of the Modern Fauna during the later Mesozoic and Cenozoic eras was paralleled by the tremendous expansion of diatoms, which are especially phosphorus-rich (via luxury storage) more so than calcareous nannoplankton[14,20,50,51]. The rain of phosphorus-rich dead organic matter likely promoted phosphorus bio-limitation in the marine realm. These trends are accompanied by a similar rise of both biogenic and total PAR; total PAR may also partly reflect authigenic phosphorus precipitation during the last 15 myr of the Neogene (Fig. 2)[52].

Nutrient Cycling Critical to Biodiversification

Nutrient cycling has nevertheless remained critical to continued marine diversification and the biogeochemical cycles of phosphorus during the PMeso-Cenozoic, as evidenced by increasing rates and depths of bioturbation during the Phanerozoic, especially beginning in the Mesozoic and through the Cenozoic[11-14,53-54]. Strontium isotope ratios are significantly greater for the Meso-Cenozoic than for the Paleozoic (Mann-Whitney U, $p<0.0001$, one-tailed), as are primary productivity and sulfate reduction, presumably in response to greater nutrient runoff (both Mann-Whitney U, $p<0.0268$, one-tailed; data from[12]). Rates of weathering are nevertheless geologically slow, limiting rates of nutrient input to the oceans from land and while biogenic PAR peaked in association with initial LIP emplacement and peak CO_2 concentrations, they began to decline almost immediately during the succeeding ~30 myr, as weathering inexorably slowed in response to CO_2 drawdown (Fig. 2). Rapid decay of dead organic matter and nutrient recycling via sulfate reduction resulting from primary productivity and the secondary productivity of GOR is indicated by the near mirror-image relation between $\delta^{34}S$ and $\delta^{13}C$ and their negative correlation (Fig. 2; Table 1). Negative correlations between pCO_2 and nannofossil diversification and between nannofossil diversification and $\delta^{34}S$ for both bin intervals further hint that higher pCO_2 levels in the atmosphere and oceans (via volcanism and organic matter decay) and elevated temperatures likely enhanced nannofossil dissolution, lowering calculated nannofossil diversification rates.

Angiosperm Leaf Decay Accelerated Nutrient Input to the Oceans

The overall diversity trend of Meso-Cenozoic marine biotas was paralleled by the evolution of terrestrial floras[55-56]. Mesozoic terrestrial floras were dominated by gymnosperms whereas angiosperms, which appeared no later than the Cretaceous, underwent tremendous expansion and diversification after the K-Pg boundary, supplanting gymnosperms[55,56]. Angiosperm leaf litter, especially that of woody deciduous species, tends to be relatively nutrient and phosphorus-rich and decay relatively rapidly as compared to that of gymnosperms, and herbaceous species generally do not produce litter that decomposes faster than that of woody species[57-59]. Among the angiosperms, grasses, which are silica-rich, became widespread during the last half of the Cenozoic in response to decreasing moisture levels as a result of glaciation; diatoms increase their proportions of total phytoplankton biomass and primary production whenever silica is not limiting[50-51]. Equilibrium mass balance models of silicate weathering by volcanic outgassing of CO_2 nevertheless indicate that increased burial of organic carbon and nutrients on land decrease weathering rates while global soil shielding reduces chemical weathering fluxes by approximately 44%, both potentially necessitating increased nutrient recycling on land[32,60]. Bedrock lithology (e.g., presence of mafic volcanics), temperature, slope gradient, runoff and water-rock contact time also play important roles in weathering rates, however[31,32]. In general, islands with high mountains, arc areas, or areas of active volcanism contribute considerably above average to runoff, chemical weathering fluxes, phosphorus and dissolved silica runoff, as well as nutrient-enriched submarine groundwater discharge (SGD)[31,61]. Tropical forested regions like those of Southeast Asia, Indonesia, and nearby archipelagoes, with their high runoff, SGD, lush rainforests, and tremendous diversity but greater shielding by nutrient-poor soils, for example, are reported as “hotspots” for chemical weathering and the runoff of phosphorus, silica, and major cations, surpassing all other regions examined[30,31,61].

Paleozoic Faunas Were Nutrient-Limited

Our results hold implications for the Paleozoic for which records are admittedly less detailed. In contrast to the Meso-Cenozoic, the early-to-middle Paleozoic portion of the diversity curve was punctuated by widely-separated peaks associated with peak

strontium isotope ratios and orogeny (Fig. 1). The eruption of continental LIPs is also thought to have been less frequent during the Paleozoic[5,34]. Although the accuracy of the LIP record before ~200 Ma is limited by the much greater duration of time available for erosion, Paleozoic LIPs are still recognizable by such features as dike swarms, and phosphorus-input has been implicated in Late Ordovician marine biotic turnover[22,28]. The earlier Paleozoic was also characterized by terrestrial floras consisting of relatively primitive, rootless and shallow-rooting taxa; the litter of modern representatives of these taxa decays relatively slowly[55-59].

These developments were paralleled by the plankton. Acritarchs were the dominant phytoplankton of the early-to-middle Paleozoic according to the fossil record and represent the organic-walled fraction of the phytoplankton preserved as cysts (resting stages resistant to inimical conditions). Acritarchs have been allied with eukaryotic “green” phytoplankton lineages, modern representatives of which are characterized by both the trace elements incorporated into their plastids that differ from those of red lineages and by high C:P ratios (low phosphorus content, carbon-rich) that would have limited biodiversification according to ecologic stoichiometric theory[20,29]. Acritarchs may represent pre-dinoflagellate lineages or perhaps even dinoflagellates themselves based on biomarkers, whereas modern dinoflagellates appear to be intermediate between red and green lineages with regard to C:P ratios[20,62]. Acritarchs largely disappeared from the fossil record during the widespread Permo-Carboniferous orogenies associated with the formation of Pangea and the spread of deeper-rooting terrestrial floras inland that is thought to have encouraged an increase of weathering rates and nutrient runoff, as indicated by strontium and selenium isotopes and phosphorus concentrations in shales, even as forests sequestered increasing amounts of carbon on land and pumped oxygen into the atmosphere (Fig. 2)[19,63,64]. Molecular clocks and reports of enigmatic calcareous microfossils suggest that calcareous plankton may have also been present early in the Paleozoic, but the extremely sporadic nature of their fossil record suggests that their populations may have been severely nutrient-limited or typically dissolved by a shallow CCD or ocean acidification resulting from high atmospheric CO_2 levels[14,65].

Is Marine Biodiversity Bounded or Unbounded?

Our results also hold implications for ecological and evolutionary theory in terms of bounded or unbounded diversification[66,67]. The Permo-Carboniferous appears transitional between the earlier Paleozoic and the Mesozoic in terms of nutrient availability, primary productivity, and the diversification of marine biotas by increasing the ability of ecosystems to sustain higher but still optimal levels of diversity[13,14,68,69]. As compared to nutrient-enrichment experiments in modern ecosystems and mass and minor extinctions, which initially lower diversity via eutrophication, the geologically-slow nutrient inputs maintain the relative stability of trophic resources in sufficient quantity thought critical to biodiversity and biodiversification, as opposed to eutrophication associated with mass extinction[12,13,22,28,70,71]. The exact pathways by which trophic resources are transmuted into biological diversity remain poorly-understood but nutrient availability and productivity undoubtedly play significant roles on different time scales, possibly through such mechanisms as enhanced metabolism and increased predation, which would have impacted biogeochemical cycles, enhanced resources available for reproduction and population increase and dispersal leading to genetic isolation, and life cycle changes[8,9,29,69]. Productivity, which would influence total PAR, oxygenation, carbon burial and sulfate reduction, has been found to increase niche diversity more than the impact of area alone on habitat diversity; this may result from: novel ecological opportunities arising more quickly with primary productivity than with area alone while higher resource density may allow for increased specialization along a resource axis while still maintaining minimum viable population sizes. Increases in area alone would therefore not be expected to facilitate resource specialization as much as increases in resource density[72].

References

1. Sepkoski, J. J. A factor analytic description of the Phanerozoic marine fossil record. *Paleobiol.* **7**, 36-53 (1981).

2. Sepkoski, J. J. A compendium of fossil marine animal genera. *Bull. Amer. Paleontol.* **363** (2002).

3. Alroy, J. The shifting balance of diversity among major marine animal groups. *Science* **329**, 1191-1994 (2010).

4. Bush, A. M. & Bambach, R. K. Sustained Mesozoic-Cenozoic diversification of marine metazoa: a consistent signal from the fossil record. *Geology* **43**, 979-982 (2015).

5. Prokoph, A., Bilali, H. E. & Ernst, R. E. Periodicities in the emplacement of large igneous provinces through the Phanerozoic: Relations to ocean chemistry and marine biodiversity evolution. *Geosci. Front.* **4**, 263-276 (2014).

6. Bambach, R.K. Energetics in the global marine fauna: a connection between terrestrial diversification and change in the marine biosphere. Geobios 32, 131–144 (1999).

7. Bush, A. M. & Bambach, R. K. Paleoecologic megatrends in marine metazoa. *Ann. Rev. Earth Planet. Sci.* **39**, 241-269 (2011).

8. Vermeij, G. J. On escalation. *Ann. Rev. Earth Planet. Sci.* **41**, 1–19 (2013).

9. Bush, A. M. & Payne, J. L. Biotic and abiotic controls on the Phanerozoic history of marine animal biodiversity. *Ann. Rev. Ecol. Evol. System.* **52**, 269-289 (2021).

10. Bambach, R.K. Seafood through time: changes in biomass, energetics, and productivity in the marine ecosystem. *Paleobiology* **19**, 372–397 (1993).

11. Martin, R.E., Quigg, A. & Podkovyrov, V. Marine biodiversification in response to evolving phytoplankton stoichiometry. *Palaeogeog., Paleoclimatol., Palaeoecol.* **258**, 277-291 (2008).

12. Cárdenas, A. L. & Harries, P. J. Effect of nutrient availability on marine origination rates throughout the Phanerozoic eon. *Nat. Geosci.* **3**, 430–434 (2010).

13. Allmon, W. D. & Martin, R. E. Seafood through time revisited: the Phanerozoic increase in marine trophic resources and its macroevolutionary consequences. *Paleobiol.* **40**, 256-287 (2014).

14. Martin, R. E. & Servais, T. Review: Did the evolution of the phytoplankton fuel the diversification of the marine biosphere? *Lethaia* **53**, 5-31 (2019).

15. Edmond, J. M. Himalayan tectonics, weathering processes, and the strontium isotope record in marine limestones. *Science* **258**, 1594-1597 (1992).

16. Richter, F. M., Rowley, D. B. & DePaolo, D. J. Sr isotope evolution of seawater: the role of tectonics. *Earth Planet. Sci. Lett.* **109**, 11-23 (1992)

17. Tardy, Y., N'Kounkou, R. & Probst, J. L. The global water cycle and continental erosion during Phanerozoic time (570 my). *Amer. Jour. Sci.* **289**, 455-483 (1989).

18. Misra, S. & Froelich, P. N. Lithium isotope history of Cenozoic seawater: changes in silicate weathering and reverse weathering. *Science* **335**, 818-823 (2012).

19. Large, R., Halpin, J. A., Lounejeva, E., Danyushevsky, L., Maslennikov, V. V. et al. Cycles of nutrient trace elements in the Phanerozoic ocean. *Gondwana Res.* **28**, 1282-1293 (2015).

20. Quigg, A., Finkel, Z. V., Irwin, A. J., Rosenthal, Y. & Ho, T. Y. The evolutionary inheritance of elemental stoichiometry in marine phytoplankton. *Nature* **425**, 291-294 (2003).

21. Vermeij, G. J. Economics, volcanoes, and Phanerozoic revolutions. *Paleobiology* **21**, 125-152 (1995).

22. Botting, J.P. The role of pyroclastic volcanism in Ordovician diversification. *Geological Society of London Special Publication* **194**, 88-113 (2002).

23. Thingstad, T.F., Krom, M.D., Mantoura, R.F.C. Flaten, G.A.F. & Groom, S. Nature of phosphorus limitation in the ultraoligotrophic eastern Mediterranean. *Science* **309**, 1068-1071 (2005).

24. Duggen, S., Croot, P., Schacht, U. & Hoffmann, L. Subduction zone volcanic ash can fertilize the surface ocean and stimulate phytoplankton growth: evidence from biogeochemical experiments and satellite data. *Geophys. Res. Lett.* **34**, L01612 (2007).

25. van Helmond, N.A.G.M., Sluijs, A., Reichart, G.J., Sinninghé Damsté, J.S. & Slomp, C. P. et al. A perturbed hydrological cycle during Oceanic Anoxic Event 2. *Geology* **42**, 123–126 (2014)

26. Shen, J., Lei, Y., Algeo, T. J., Qinglai, F., Servais, T. et al. Volcanic effects on microplankton during the Permian-Triassic transition (Shangsi and Xinmin, south China). *Palaios* **28**, 552-567 (2013).

27. Percival, L. M. E., Cohen, A. S., Davies, M. K., Dickson, A. J., Hesselbo, S. et al. Osmium isotope evidence for two pulses of increased continental weathering linked to Early Jurassic volcanism and climate change. *Geology* **44**, 759-762 (2016).

28. Longman, J., Mills, B. J. W., Manners, H. R., Gernon, T. M. & Palmer, M. R. Late Ordovician climate change and extinctions driven by elevated volcanic nutrient supply. *Nat. Geosci.* **14**, 924-929 (2021).

29. Sterner, R. W. & Elser, J. J. *Ecological Stoichiometry: The Biology of Elements from Molecules*. (Princeton University Press, 2002).

30. Dessert, C., Dupré, B., Gaillardet, J., François, L. M., & Allègre, C. J. Basalt weathering laws and the impact of basalt weathering on the global carbon cycle. *Chem. Geol.* **202**, 257–273. doi: 10.1016/j.chemgeo.2002.10.001(2003).

31. Milliman, J. D. & K. L. Farnsworth, *River Discharge to the Coastal Ocean: A Global Synthesis*. (Cambridge, UK: Cambridge University Press, 2011).

32. Hartmann, J., Moosdorf, N., Lauerwald, R., Hinderer, M. & West, A. J. Global chemical weathering and associated P-release-the role of lithology, temperature and soil properties. *Chem. Geol.* **363**, 145-163 (2014).

33. Gernon, T. M., Hincks, T. K., Merdith, A. S., Rohling, E. J., Palmer, M. R. et al. Global chemical weathering dominated by continental arcs since the mid-Paleozoic. *Nat. Geosci.* **14**, 690-696 (2021).

34. Johansson, L. Zahirovic, S., & Müller, R. M. The interplay between the eruption and weathering of large igneous provinces and the deep-time cycle. *Geophys. Res. Lett.* **45**, 5380-5389 (2018).

35. Tyrrell, T. The relative influences of nitrogen and phosphorus on oceanic primary production. *Nature* **400**, 525–531 (1999).

36. Moore, C.M., Mills, M. M., Arrigo, K. R., Berman-Frank, I., Bopp, L. et al. Processes and patterns of oceanic nutrient limitation. *Nat. Geosci.* **6**, 701-710 (2013).

37. Sharoni S. & I. Halevy. Geologic controls on phytoplankton elemental composition. *Proc. Nat. Acad. Sci.* **119**, https://doi.org/10.1073/pnas.2113263118 (2022).

38. Materials and Methods are available as Supplementary Materials at the *Nature Geoscience* website.

39. Föllmi, K. B. 160 m.y. record of marine sedimentary phosphorus burial: Coupling of climate and continental weathering under greenhouse and icehouse conditions. *Geology* **23**, 859-862 (1995).

40. Miller, K. G., Kominz, M., Browning, J. V., Wright, J. D., Mountain, G. S. et al. The Phanerozoic record of global sea-level change. *Science* **310**, 1293-1298 (2005).

41. Bown, P. R., Lees, J. A. & Young, J. R. Calcareous nannoplankton diversity and evolution through time, in *Coccolithophores - From Molecular Processes to Global Impact* (eds H. Thierstein, H. & Young, J.) Chap. 18 (Springer, 2004).

42. Foster, G. L., Royer, D. L. & Lunt, D. J. Future climate forcing potentially without precedent in the last 20 million years. *Nat. Comm.* **8**, doi: ncomms14845 |www.nature.com/naturecommunications (2017).

43. Valentine, J. W. & Moores, E. M. Global tectonics and the fossil record. *Journal of Geology* **80**,167-184 (1972).

44. Martin, R. E. The fossil record of biodiversity: nutrients, productivity, habitat area and differential preservation. *Lethaia* **36**, 179-193 (2003).

45. Hannisdal, B. & Peter, S. E. Phanerozoic earth system evolution and marine biodiversity. *Science* **334**, 1121–1124 (2011).

46. Zaffos, A., Finnegan, S., Peters, S. E. Plate tectonic regulation of global marine animal diversity. *Proc. Nat. Acad. Sciences* 1**14**, 5653-5658. doi:10.1073/pnas.1702297114 (2017).

47. Roberts, G. G. & Mannion, P. D. Timing and periodicity of Phanerozoic marine biodiversity and environmental change. *Nature*. doi.org/10.1038/s41598-019-42538-7 (2019).

48. Wong, K., Mason, E., Brune, S., East, M., Edmonds, S. et al. Deep carbon cycling over the past 200 million years: a review of fluxes in different tectonic settings. *Front. Earth Sci.* **7**, doi:10.3389/feart.2019.00263 (2019).

49. Planck, T. & Manning, C. E. Subducting carbon. *Nature* **574**, 343-352 (2019).

50. Margalef, R. Life-forms of phytoplankton as survival alternatives in an unstable environment. *Oceanol. Acta* **1**, 493–509 (1978).

51. Cermeño, P. The geological story of marine diatoms and the last generation of fossil fuels. *Perspect. Phycol.* **2**, 53–60 (2016).

52. Anderson, L. D., Delaney, M. L. & Faul, K. L. Carbon to phosphorus ratios in sediments: implications for nutrient cycling. *Glob. Biogeochem. Cycles* **15**, 65–79 (2001).

53. Thayer, C. W. Sediment-mediated biological disturbance and the evolution of marine benthos. in *Biotic Interactions in Recent and Fossil Benthic Communities* (eds Tevesz, M.J.S. & McCall, P.L.) Chapter (Plenum,1983).

54. van Mooy, B.A.S., Krupke, A., Dyhrman, S.T., Fredricks, H.F., Frischkorn, K.R. et al. Major role of planktonic phosphate reduction in the marine phosphorus redox cycle. *Science* **348**, 783–785 (2015).

55. Cleal, C. J. & Cascales-Miñana, B. Composition and dynamics of the great Phanerozoic evolutionary floras. *Lethaia* **47**, 469–484 (2014).

56. Dahl, T. W. & Arens, S. K. M. The impacts of land plant evolution on Earth's climate and oxygenation state – An interdisciplinary review. *Chemical Geology* **547**, doi.org/10.1016/j.chemgeo.2020.119665 (2020)

57. Wright, I. J., Reich, P. B., Ackerly, D. D., Baruch, Z., Bongers, F. et al. The worldwide leaf economics spectrum. *Nature* **428**, 821-827 (2004).

58. Cornwell, W. K., Cornelissen, J. H. C., Amatangelo, K., Dorrepaal, E., Eviner, V. T. et al. Plant species traits are the predominant control on litter decomposition rates within biomes worldwide. *Ecol. Lett.* **11**, 1065–1071 (2008).

59. Díaz, S., Kattge, J., Cornelissen, J. H. C., Wright, I. J., Lavore, S. et al. The global spectrum of plant form and function. *Nature* **529**, 167-171 (2016).

60. D'Antonio, M P., Ibarra, D. E. & Boyce, C. K. Land plant evolution, decreased, rather than increased weathering rates. *Geology***48**, 29-33.

61. Zhou, Y.-Q., Sawyer, A. H., David, C. H. & Famiglietti, J. S. Fresh submarine groundwater discharge to the near-global coast. *Geophys. Res. Lett.* **46**, 5855-5863 (2019).

62. Moldowan, J. M. & Talyzina, N. M. Biogeochemical evidence for dinoflagellate ancestors in the Early Cambrian. *Science* **281**, 1168–1170 (1998).

63. Servais, T., Martin, R. E. & Nützel, A. The impact of the 'terrestrialization process' in the late Palaeozoic: pCO2, pO2, and the 'phytoplankton blackout'. *Rev. Palaeobot. Palynol.* **224**, 26–37 (2016).

64. Algeo, T. J. & Scheckler, S. E. Terrestrial-marine teleconnections in the Devonian: links between the evolution of land plants, weathering processes, and marine anoxic events. *Philosoph. Trans.Roy. Soc. London* **B353**, 113-130 (1998).

65. Munnecke, A. & Servais, T. Palaeozoic calcareous plankton: evidence from the Silurian of Gotland. **Lethaia** *41*, 185–194 (2008).

66. Rabosky D. L. & Hurlbert, A. H. Species richness at continental scales is dominated by ecological limits. *Amer. Natural.* **185**, 572-583 (2015).

67. Harmon, L. J. & Harrison, S. Species diversity is dynamic and unbounded at local and continental scales. *Amer. Natural.* **185**, 584-593 (2015).

68. Rosenzweig, M L. & Abramsky, Z. How are diversity and productivity related? in *Species Diversity in Ecological Communities: Historical and Geographical Perspectives* (eds Ricklefs, R. E. & Schluter, D.) Chap. 5 (University of Chicago Press, 1993).

69. Antell, G. W. & Saupe, E. E. Bottom-up controls, ecological revolutions and diversification in the oceans through time. *Curr. Biol.* **31**, R1237-R1251. https://doi.org/10.1016/j.cub.2021.08.069 (2021).

70. Martin, R.E. Catastrophic fluctuations in nutrient levels as an agent of mass extinction: upward scaling of ecological processes? in *Biodiversity Dynamics: Turnover of Populations, Taxa, and Communities* (eds McKinney, M.L. & Drake, J.A.) Chap. 17 (Columbia University Press, 1998).

71. Algeo, T. J., Chen, Z. Q., Fraiser, M. L., & Twitchett, R. J. Terrestrial–marine teleconnections in the collapse and rebuilding of Early Triassic marine ecosystems. *Palaeogeog., Palaeoclimatol., Palaeoecol.* **308**, 1-11 (2011).

72. Hurlbert, A. H. & Stegen, J. C. When should species richness be energy limited, and how would we know? *Ecol. Lett.* **17**, 401-413 (2014).

Methods

Materials. Data was compiled from a range of sources, which used various time scales and bins. See Supplementary Table S1 and Supplementary Fig. S1 for their raw data with their originally assigned ages.

Data used by Cárdenas and Harries[12] were initially binned to 5-myr intervals using Linear Interpolation, including Genera Origination Rate (GOR) data of Alroy[73] reported by him in approximately 11-myr bins. All data were then re-binned to 11-myr bins by Cardenas and Harries[12], mirroring those used in the calculation of origination rates by Alroy[73], prior to undertaking their statistical analyses. Materials sources are indicated below.

1) Strontium isotope ratios (‰)[12]: Data originally from McArthur et al.[74] and linearly interpolated by Cárdenas and Harries[12] in even 5-myr intervals recalibrated by them to the GTS2004 time scale[75], and then re-binned to approximate 5-myr intervals by Cárdenas and Harries[12].

2) CO_2 (ppm[42]): Compiled from various sources and reported at various time intervals. Ages updated to GTS2012 time scale[76].

3) Average Phosphorus Accumulation Rates (PAR, mg□cm^{-2} ka^{-1})[39]: Reported at 0.5 myr intervals beginning at 0.5 Ma based on a global data base of Deep Sea Drilling Project (DSDP) and Ocean Drilling Project (ODP) cores. Ages were attributed to each measurement using recent biostratigraphic distribution charts and the time table of Harland et al.[77] by Föllmi[39].

Two time series were examined by us: Biogenic and Total (Biogenic + "Detrital"). Total PAR data extend back to 159.5 Ma (Jurassic, ca. late Oxfordian), Detrital to 102.5 Ma, and Biogenic to 100.5 Ma (Cretaceous, late Albian). The total P dataset includes information on phosphate phases that were originally dissolved and bioavailable and those that were detrital, i.e., derived from continental weathering without intermittent biological involvement. Föllmi attempted to discriminate between these two phases by considering a subset of pelagic biogenic sediments[39]. Phosphorus phases in this data subset were considered by him to likely be mainly nondetrital and representing reactive bioavailable phosphorus. The similarity of the total PAR and biogenic PAR curves (Fig. 2) indicates that changes in total P fluxes were closely tracked by changes in biogenic PAR fluxes or, perhaps more generally according to Föllmi, that changes in total continental weathering rates led to comparable changes in chemical weathering as the main long-term source of dissolved bioavailable phosphorus, i.e., that changes in total continental weathering rates led to comparable changes in chemical weathering rates as the main long-term source of dissolved bioavailable phosphorus[39].

4) Carbon isotope ratios ($\delta^{13}C$, ‰)[12]: Data originally from Veizer et al.[78]. Data were treated by Cárdenas and Harries as for Sr isotope ratios[12]. Enhanced productivity is reflected as an increase in carbon isotope ratios, whereas decreased productivity or the oxidation or input of dead organic matter are registered as lower ratios.

5) Sulfur isotope ratios ($\delta^{34}S$, ‰)[12]: Data originally from Kampschulte and Strauss in 5-myr intervals[79]. Data treated by Cárdenas and Harries as above[12]. Enhanced rates of bacterial sulfate reduction register as an increase in sulfur isotope ratios ($\delta^{34}S$) while those of carbon ($\delta^{13}C$) decrease in response to the concomitant release of its lighter isotope that results from the destruction of organic matter by sulfate-reducing bacteria.

6) Sea-level (meters)[40]: Used by Cárdenas and Harries and originally reported on various durations based on GTS2004 time scale and re-binned by them[12, 75].

7) Calcareous nannoplankton diversification rates[41]: Available as graphs on 3-myr intervals and expressed as percentage increase or decrease of Rate of Speciation (R_s) – Rate of Extinction (R_e). Data were originally plotted as id-points of intervals calibrated according to Berggren et al. and Gradstein et al. [80,81]. Peaks and valleys of Bown et al.'s Figure 3 were digitized by us, resulting in data points spaced ~3 myr apart[41,82].

8) Genera Origination Rates[12]: Data originally from Alroy on approximate 11-myr intervals based on GTS2004 time scale, then re-binned by Cárdenas and Harries to ~5-myr intervals, and re-binned by us to uniform 5-myr intervals[12,73,75]. Alroy originally binned marine origination rates using the global compilation of the Paleobiology Database into 48 intervals averaging 11 myr in duration and calibrated to the GTS2004 time scale[73].

9) Large Igneous Provinces (LIP, km^2)[34]: Data reported on 1-myr intervals and shown herein in Fig. 2. These data were not used in correlations because of numerous zero values (Fig. 2; Table 1).

Statistical Analysis. We first conducted statistical analyses in Paleontological Analysis Statistical Software (PAST) version 4.03 and reaffirmed the results in R[83,84]. Linear Interpolation was used by us to re-bin all original data to 5-myr intervals approximately midway between 11-myr bins intervals in an attempt to achieve greater temporal resolution while remaining within the temporal constraints of the raw data. In several cases for data not taken from Cárdenas and Harries[12], we readjusted the youngest ages to exactly 17 Ma so as to obtain exactly uniform 11-myr bins and from which we produced uniform 5-myr bins via linear interpolation. Readjusted ages (see below for original sources) are for: CO_2 (originally 17.5 Ma), Phosphorus Accumulation Rate (PAR, total and biogenic; originally 17.5 Ma) and nannofossil diversification rates (originally 17.788 Ma; Supplementary Tables S2-S3; Supplementary Figs. S2, S3).

Data were then differenced to eliminate possible spurious correlations using the Evaluation Expression (u-d) of the Transform Data option of PAST (i.e., the value of each interval was subtracted from the one succeeding it in time; Supplementary Tables S4, S5; Supplementary Figs. S4, S5). Due to the non-normal distributions of the original data sets (Normality Tests option under PAST Univariate menu), we then correlated using Spearman's coefficient. Individual time series vary slightly in length; consequently, correlations were conducted only as far back in age as comparisons with the PAR time series permitted: ~159 Ma (Supplementary Fig. S6) [39].

We correlated both 11- and 5-myr binned uncorrected data and the same data corrected with the Bonferroni procedure. The Bonferroni correction has been widely recommended when conducting multiple comparisons to cull null hypotheses which should be rejected, but it has also been severely criticized, as it is extremely conservative. As the number of variables used in comparisons increases, the required p value with the Bonferroni correction for the rejection of the null hypothesis becomes increasingly small to the point that it may begin to produce false negatives (Type I error: null hypothesis rejection) rather than omitting false positives (Type II error: null hypothesis acceptance)[85-87]. Some workers therefore advocate using only uncorrected data for this reason[86-87]. The Bonferroni correction is based on the equation p (corrected) = α/m, where α = desired uncorrected p at the outset (e.g., 0.05 in our study) and m = number of comparisons ("hypotheses" to be tested). In our study, requiring a normal p value of 0.05 and including all variables in comparisons with a Bonferroni correction required a p value of 0.0014 (0.05/36); this resulted in no correlations for 11-myr binned data and only one significant correlation, that between biogenic PAR and GOR, for 5-myr binned data ($\rho \approx 0.92$; $p < 3.2E\text{-}05$). We previously established that CO_2 and sea level did not correlate with GOR using uncorrected data. We therefore chose to eliminate these two variables to further test the strength of correlations of biogeochemical indices with GOR and each other, and which had previously yielded significant correlations with uncorrected 5-myr binned data (Table 1). Elimination of CO_2 and sea level resulted in a somewhat higher p value of 0.0024 (p = 0.05/21 comparisons) for the correlation of corrected data.

References

73. Alroy, J. Dynamics of origination and extinction in the marine fossil record. *Proc. Natl. Acad. Sci. U.S.A.* **105**, 11536-11542 (2008).

74. McArthur, J. M., Howarth, R. J. & T. R. Bailey, Strontium isotope stratigraphy: LOWESS version 3: Best fit to the marine Sr-isotope curve for 0-509 Ma and accompanying look-up table for deriving numerical age. *Jour. Geol.* **109**, 155-170 (2001).

75. Gradstein, F. M., Ogg, J. G. & Smith, A. G. Eds., *A Geologic Time Scale*, *2004* (Cambridge University Press, 2004).

76. Gradstein, F. M., Ogg, J. G., Schmitz, M. D. & Ogg, G. M. Eds., *The Geologic Time Scale* (Elsevier, 2012).

77. Harland, W. B., Armstrong, R. L., Cox, A. V., Craig, L. E., Smith, A. G. et al. *A Geological Timescale 1989* (Cambridge University Press, 1990).

78. Veizer, J., Davin, A., Azmy, K., Bruckschen, P., Buhl, D. et al. $^{87}Sr/^{86}Sr$, $\delta^{13}C$ and $\delta^{18}O$ evolution of Phanerozoic seawater. *Chem. Geol.* **161**, 59-88 (1999).

79. Kampschulte, A. & Strauss, H. The sulfur isotopic evolution of Phanerozoic seawater based on the analysis of structurally substituted sulfate in carbonates. *Chem. Geol.* ***204***, 255-286 (2004).

80. Berggren, W. A., Kent, D. V., Swisher III, C. C. &Aubry, M.-P., A revised Cenozoic chronology and chronostratigraphy in *Geochronology, Time-Scales, and Global Stratigraphic Correlation: Framework for an Historical Geology* (eds. Berggren, W. A., Kent, D. V. & Hardenbol, J.) Chap. 8 (Society for Sedimentary Geology, 1995).

81. Gradstein, F. M., Agterberg, F. P., Ogg, J. G., Hardenbol, J., Van Veen, P. et al. A Triassic, Jurassic and Cretaceous time-scale, in *Geochronology, Time-Scales, and Global Stratigraphic Correlation:Framework for an Historical Geology* (eds W. A. Berggren, W. A., Kent, D. V. & Hardenbol, J.) Chap. 7 (Society for Sedimentary Geology, 1995)

82. Rohatgi, A. C:\Users\Carol\Desktop\WebPlotDigitizer-4.2-win32-x64.

83. Hammer, Ø. https://past.en.lo4d.com/windows

84. The R Project for Statistical Computing, www.r-project.org.

85. Rothman, K. J., No adjustments are needed for multiple comparisons. *Epidemiology* **1**, 43-46 (1990).

86. Perneger, T. V. What is wrong with Bonferroni adjustments. *Brit. Med. Jour.* **136**, 1236-1238 (1998).

87. Cabin, R. J. & Mitchell, R.J. To Bonferroni or not to Bonferroni: when and how are the questions. *Bull. Ecol. Soc. Amer.* **81**, 246-248 (2000).

Declarations

Acknowledgments

Thomas Servais reviewed and commented on a late draft of the manuscript.

Author contributions

REM conceived the project. Both authors contributed to the methods, analysis, and writing.

Competing interests

Authors declare no competing interests.

Data and materials availability

All data are available in the main text or the supplementary materials online.

Figures

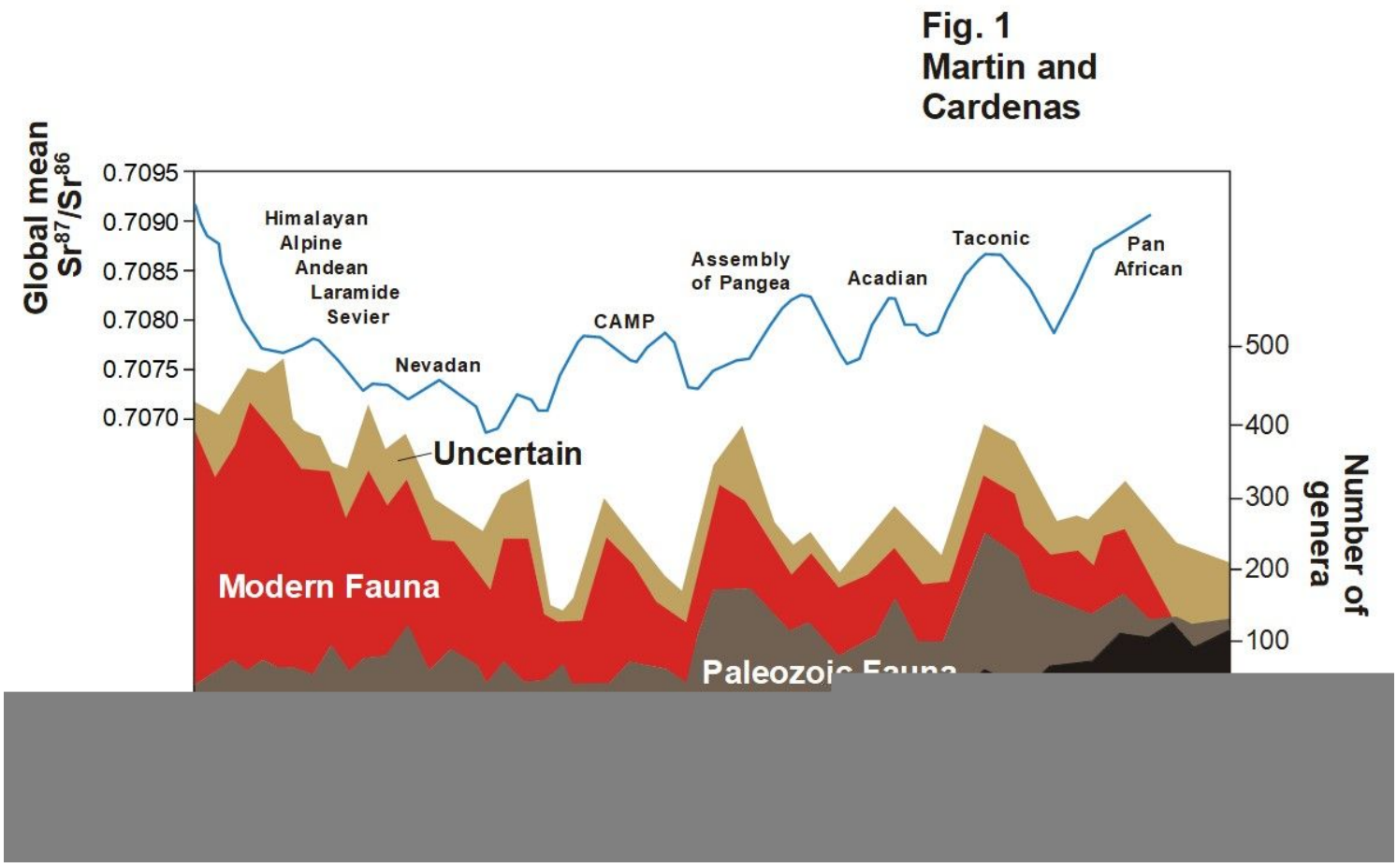

Figure 1

Marine biodiversity and orogeny during the Phanerozoic Eon. Genus-level richness (redrawn from 3, based on 2) with strontium isotope ($^{87}Sr/^{86}Sr$) curve (at 1 myr intervals[5]). Major orogenic episodes for the Phanerozoic are indicated. CAMP = Central Atlantic Magmatic Province.

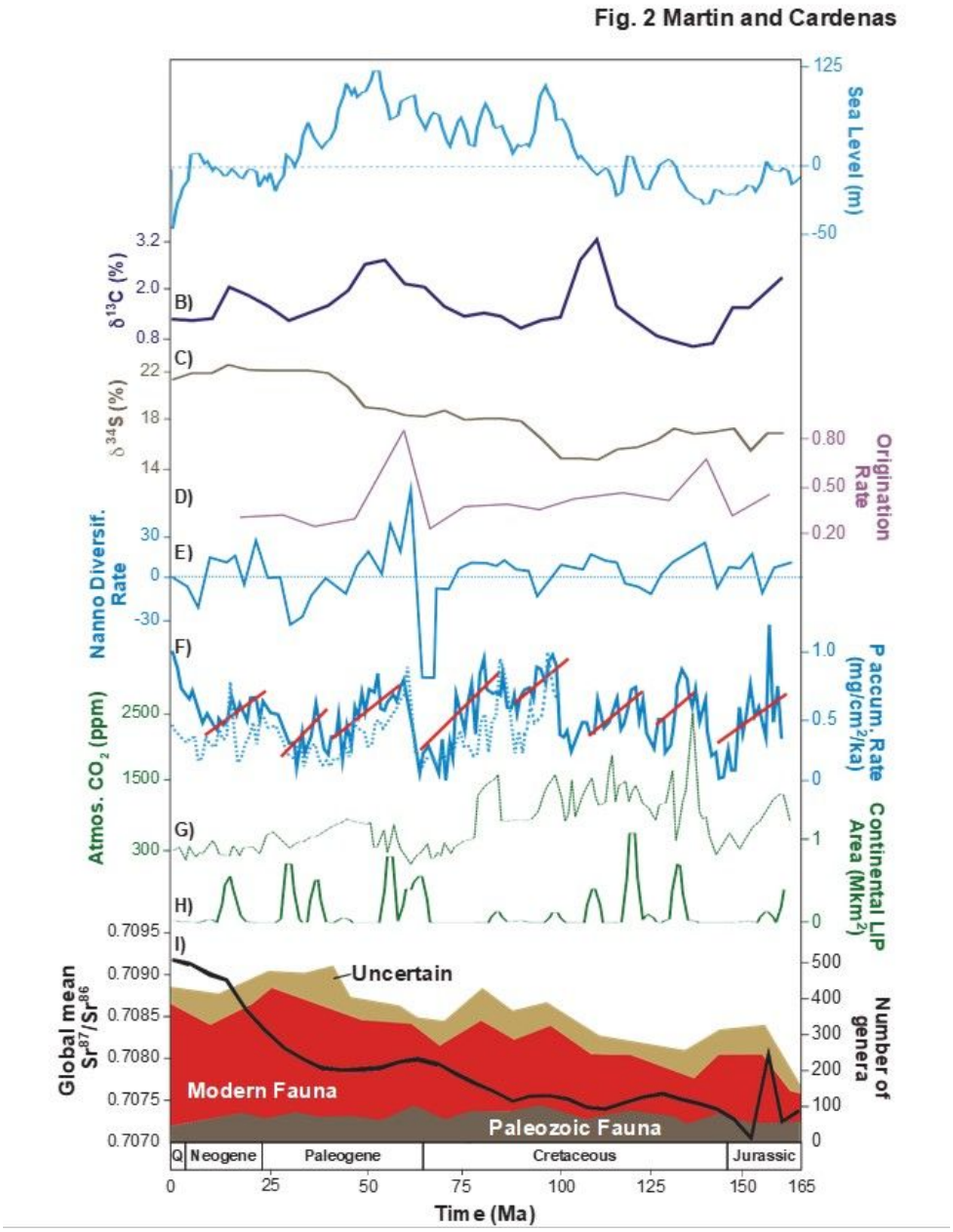

Figure 2

Physical, biogeochemical, and diversity indices for the Phanerozoic. a, Sea level[40]. **b**, $\delta^{13}C$[12]. **c**, $\delta^{34}S$[12]. **d**, Origination rate[12]. **e,** Nannofossil diversification rate41. **f,** Phosphorus accumulation rates (PAR)[39]. Solid line: total (biogenic + detrital) rate. Dashed line: biogenic rate only. Solid lines indicate generally declines in PAR and CO_2 following Large Igneous Province (LIP) emplacement. Original PAR outlier value at 0.5 Ma removed for sake of scale (see Supplementary Information). **g**, Carbon dioxide levels[42]. **h**, Area of continental Large Igneous Province (LIP) emplacement[34]. **i**, Meso-Cenozoic genera biodiversity from Fig. 1 and strontium isotope ratios in approximate 5-myr bins[12].

Supplementary Files

This is a list of supplementary files associated with this preprint. Click to download.

- SupplementaryFiguresandTables.docx